Proceedings of the 2016 IEEE/SICE International Symposium on System Integration, Sapporo Convention Center, Sapporo, Japan, December 13-15, 2016

Dynamical Model of Humanoid Considering Slipping with Nonlinear Floor Friction and Internal Force During Free-fall Motion

Xiang Li, Daiji Izawa, Mamoru Minami, Takayuki Matsuno[1] and Akira Yanou[2]

Abstract— **Biped locomotion created by controlling me- thods based on Zero-Moment Point (ZMP) has been realized in real world and been well verified its efficacy for stable walking. However the walking strategies that have been proposed so far seem to avoid such considerations as slipping of foot on the floor, even though there should exist the slipping large or small in real world. In this research, a dynamical model of humanoid robot including slipping of foot is proposed, which is derived by the Newton-Euler (NE) method. To confirm the veracity of the derived dynamicl model, the model has been verified from the view point that when all friction coefficients are identical to zero, the total kinetic energy should be conserved to be unchanged, and when the coefficients are not zero, the total kinetic energy should decrease monotonously.**

I. INTRODUCTION

Human beings have acquired an ability of stable bipedal walking in evolving so far in a repetition of generation. From a view point of making a stable controller for the bipedal walking based on knowledge of control theory, it looks not easy because of the complicated dynamics with high nonlinearity and coupled interactions between state variables with high dimensions. Therefore how to simplify the complicated walking dynamics to help construct stable walking controller has been studied intensively.

Avoiding complications in dealing directly with true dynamics without approximation, inverted pendulum has been used frequently for making a controller[1]-[3], by using the merits to simplify the calculations to determine control input torque. Further, linear approximation that makes the humanoid model represented by simple inverted pendulum enables researchers to realize stable gait through well-known control strategy[4]-[6] since these researches include assumptions justifying the approximations, the hypotheses leave obscureness in the discussions of the robot's dynamical behaviors.

Our research has begun from similar view point of [7], [8] as aiming to describing gait's dynamics as correctly as possible, including slipping of foot on the floor, with whole body humanoid dynamics consisted of head, waist, torso, arms and legs. And that what the authors think more important is that the dimension of dynamical equation will change depending on the walking gait's varieties, which has been discussed in [9] by using one legged hopping robot. In fact, this kind of dynamics with the dimension number of state variables varying by the result of its dynamical time transitions are out of the arena of control theory that discusses how to control a system with fixed states' number. Further the tipping over motion has been called as non-holonomic dynamics that includes a joint without inputting torque, i.e., free joint that is rotation of toe when walking and especially stumbling. Landing of the heel or the toe of lifting leg in the air to the ground makes a geometrical contact[10] and the contact gives a constraint condition to the humanoid's dynamics.

The conventional NE method could be applied only to a robot having an open loop serial linkage structure, therefore the dynamical model of robots made by NE method was limited within a condition that the robot does not contact external world. Therefore the NE method has not been utilized for modeling of robots that works under a premise that it contacts with the environment, e.g., when the robot conducts some grinding task or assembling task. In order to eliminate this limitation, one of authors has proposed Extended NE (ENE) method [11] that could be utilized for dynamical modeling of manipulator whose hand is kinematically constraint by non-elastic environment. This method utilizes recursive calculation of accleration and exerting force/torque along to the robot's serial link stracture including inner force/torque and that this is important merit of the ENE that Lagrange Method does not have. The demerit of ENE is that the constraint force exerting between the robot and the environment should be predetermined before recursive calculation starts. Averting the demerit of the ENE, it is convenient to deal with the constraint motion problem by solving robot's angular acceleration and contacting force through simultaneous equation, which has been introduced by [12] and published in a book [13]. Then the simultaneous solving method [13] of the acceleration and contacting force has been used for describing the humanoid's walking dynamics with contacting constraints over the external environments, which is in this paper the floor on which the humanoid walks.

In this research that based on [14][15], a walking model of humanoid robot including slipping, bumping, surface-contacting and point-contacting of foot is discussed, and its dynamical equation is derived by the NE method. Especially the common consideration of the free-leg model [16]–[18] is without any slipping. Additionally, this research is different from the previous humanoid researches [19]–[22], on the point that nonlinear friction including the stick/slip friction is discussed in walking motion of humanoid robot consisting of 17 rigid links. [19], [20] are the experimental discussions on walking with slippage. And [21], [22] have tried to discuss

[1]Graduate School of Nature Science and Technology, Okayama University, 3-1-1 Tsushima-naka, Kita-ku, Okayama, 700-8530, Japan pzkm87r2@s.okayama-u.ac.jp

[2]Department of Radiological Technology, Kawasaki College of Allied Health Professions, Kurashiki, Okayama, 701-0194, Japan yanou-a@mw.kawasaki-m.ac.jp

978-1-5090-3328-7/16/$31.00 ©2016 IEEE

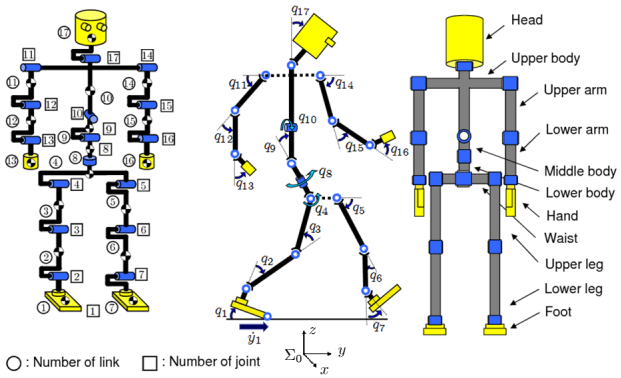

Fig. 1. Definition of humanoid's link, joint and whole body.

TABLE I

PHYSICAL PARAMETERS.

Link	Link number	l_i[m]	m_i[kg]	d_i[Nms/rad]
Head	17	0.24	4.5	0.5
Upper body	10	0.41	21.5	10.0
Middle body	9	0.1	2.0	10.0
Lower body	8	0.1	2.0	10.0
Upper arm	11, 14	0.31	2.3	0.03
Lower arm	12, 15	0.24	1.4	1.0
Hand	13, 16	0.18	0.4	2.0
Waist	4	0.27	2.0	10.0
Upper leg	3, 5	0.38	7.3	10.0
Lower leg	2, 6	0.40	3.4	10.0
Foot	1, 7	0.07	1.3	10.0
Total weight [kg]		—	64.2	—
Total hight [m]		1.7	—	—

the influences of stick/slip slipping states during walking, however those papers lack description of relations between full body dynamical model and the stick/slip slippage of foot. Therefore how the dynamical effects of stick/slip have been incorporated into the whole body dynamics is not explained.

In this paper, a dynamical model of humanoid including influences of nonlinearity caused by stick-slip [23]–[25] motions, which are derived from the nonlinear friction between the floor and humanoid's feet, is introduced and the stick/slip effect is intensively discussed.

In the stick/slip simulation of this paper, the body of humanoid will do the free-fall motion. Free-fall motion is a very dangerous pattern for the humanoid robot. Because during the free-fall motion, the internal force in some joints become very large. When the internal force is lager than the limit. The joints or structure of robot will be broken. In this paper, the internal force during free-fall motion will be discussed. The internal force can be calculated by NE method that is one of the merits of the NE method.

II. DYNAMICAL WALKING MODEL

A. Forward kinematical calculations

We discuss a biped robot whose definition is depicted in Fig.1. Table I indicates length l_i [m], mass m_i [kg] of links and coefficient of joints' viscous friction d_i [N·m·s/ rad], which are decided based on [27]. This model is simulated as a serial-link manipulator having ramifications and represents rigid whole body—feet including toe, torso, arms and so on—by 17 degree-of-freedom. Though motion of legs is restricted in sagittal plane, it generates varieties of walking gait sequences since the robot has flat-sole feet and kicking torque. In this paper, one foot including link-1 is defined as "supporting-leg" and another foot including link-7 is defined as "free-leg" ("contacting-leg" when the free-leg contacts with floor) according to the walking state.

In this paper, we derive the equation of motion following by NE formulation. So we must consider the structure of the supporting-leg with two situations. When the supporting-leg is constituted by rotating joint: We first have to calculate relations of positions, velocities and accelerations between links as forward kinetics procedures from bottom link to top link. Serial link's angular velocity ${}^i\boldsymbol{\omega}_i$, angular acceleration ${}^i\dot{\boldsymbol{\omega}}_i$, acceleration of the origin ${}^i\ddot{\boldsymbol{p}}_i$ and acceleration of the center of mass ${}^i\ddot{\boldsymbol{s}}_i$ based on Σ_i fixed at i-th link are obtained as follows.

$$ {}^i\boldsymbol{\omega}_i = {}^{i-1}\boldsymbol{R}_i^T\ {}^{i-1}\boldsymbol{\omega}_{i-1} + \boldsymbol{e}_{z_i}\dot{q}_i \tag{1} $$

$$ {}^i\dot{\boldsymbol{\omega}}_i = {}^{i-1}\boldsymbol{R}_i^T\ {}^{i-1}\dot{\boldsymbol{\omega}}_{i-1} + \boldsymbol{e}_z\ddot{q}_i + {}^i\boldsymbol{\omega}_i \times (\boldsymbol{e}_{z_i}\dot{q}_i) \tag{2} $$

$$ \begin{aligned} {}^i\ddot{\boldsymbol{p}}_i = {}^{i-1}\boldsymbol{R}_i^T \Big\{ & {}^{i-1}\ddot{\boldsymbol{p}}_{i-1} + {}^{i-1}\dot{\boldsymbol{\omega}}_{i-1} \times {}^{i-1}\hat{\boldsymbol{p}}_i \\ & + {}^{i-1}\boldsymbol{\omega}_{i-1} \times ({}^{i-1}\boldsymbol{\omega}_{i-1} \times {}^{i-1}\hat{\boldsymbol{p}}_i) \Big\} \end{aligned} \tag{3} $$

$$ {}^i\ddot{\boldsymbol{s}}_i = {}^i\ddot{\boldsymbol{p}}_i + {}^i\dot{\boldsymbol{\omega}}_i \times {}^i\hat{\boldsymbol{s}}_i + {}^i\boldsymbol{\omega}_i \times ({}^i\boldsymbol{\omega}_i \times {}^i\hat{\boldsymbol{s}}_i) \tag{4} $$

Then if the supporting-leg is constituted by prismatic joint. We will switch the equations as the following.

$$ {}^i\boldsymbol{\omega}_i = {}^{i-1}\boldsymbol{R}_i^{\mathrm{T}}\ {}^{i-1}\boldsymbol{\omega}_{i-1} \tag{5} $$

$$ {}^i\dot{\boldsymbol{\omega}}_i = {}^{i-1}\boldsymbol{R}_i^{\mathrm{T}}\ {}^{i-1}\dot{\boldsymbol{\omega}}_{i-1} \tag{6} $$

$$ \begin{aligned} {}^i\ddot{\boldsymbol{p}}_i = {}^{i-1}\boldsymbol{R}_i^{\mathrm{T}} \Big\{ & {}^{i-1}\ddot{\boldsymbol{p}}_{i-1} + {}^{i-1}\dot{\boldsymbol{\omega}}_{i-1} \times {}^{i-1}\hat{\boldsymbol{p}}_i \\ & + {}^{i-1}\boldsymbol{\omega}_{i-1} \times ({}^{i-1}\boldsymbol{\omega}_{i-1} \times {}^{i-1}\hat{\boldsymbol{p}}_i) \Big\} \\ & + 2({}^{i-1}\boldsymbol{R}_i^{T\,i-1}\boldsymbol{\omega}_{i-1}) \times (\boldsymbol{e}_z\dot{q}_i) + \boldsymbol{e}_z\ddot{q}_i \end{aligned} \tag{7} $$

$$ {}^i\ddot{\boldsymbol{s}}_i = {}^i\ddot{\boldsymbol{p}}_i + {}^i\dot{\boldsymbol{\omega}}_i \times {}^i\hat{\boldsymbol{s}}_i + {}^i\boldsymbol{\omega}_i \times ({}^i\boldsymbol{\omega}_i \times {}^i\hat{\boldsymbol{s}}_i) \tag{8} $$

Here, ${}^{i-1}\boldsymbol{R}_i$ means orientation matrix, ${}^{i-1}\hat{\boldsymbol{p}}_i$ represents position vector from the origin of $(i-1)$-th link to the one of i-th, ${}^i\hat{\boldsymbol{s}}_i$ is defined as gravity center position of i-th link and $\boldsymbol{e}_{z_i}$ is unit vector that shows rotational axis of i-th link. However, velocity and acceleration of 4th link transmit to 8th link and ones of 10th link transmit to 11th, 14th and 17th link directly because of ramification mechanisms.

B. Backward inverse dynamical calculations

After the above forward kinetic calculation has been done, contrarily inverse dynamical calculation from top to base link are shown as follow. Newton equation and Euler equation of i-th link are represented by Eqs.(9), (10) when ${}^i\boldsymbol{I}_i$ is defined as inertia tensor of i-th link. Here, ${}^i\boldsymbol{f}_i$ and ${}^i\boldsymbol{n}_i$ in Σ_i show the force and moment exerted on i-th link from (i+1)-th link.

$$
\begin{aligned}
{}^i\boldsymbol{f}_i &= {}^i\boldsymbol{R}_{i+1}{}^{i+1}\boldsymbol{f}_{i+1} + m_i{}^i\ddot{\boldsymbol{s}}_i \qquad (9)\\
{}^i\boldsymbol{n}_i &= {}^i\boldsymbol{R}_{i+1}{}^{i+1}\boldsymbol{f}_{i+1} + {}^i\boldsymbol{I}_i{}^i\dot{\boldsymbol{\omega}}_i + {}^i\boldsymbol{\omega}_i \times ({}^i\boldsymbol{I}_i{}^i\boldsymbol{\omega}_i)\\
&\quad + {}^i\hat{\boldsymbol{s}}_i \times (m_i{}^i\ddot{\boldsymbol{s}}_i) + {}^i\hat{\boldsymbol{p}}_{i+1} \times ({}^i\boldsymbol{R}_{i+1}{}^{i+1}\boldsymbol{f}_{i+1}) \qquad (10)
\end{aligned}
$$

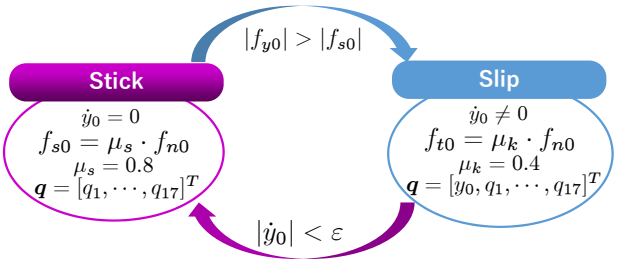

Fig. 2. Switch conditions of stick-slip motion.

On the other hand, since force and torque of 5th and 8th links are exerted on 4th link, effects onto 4th link as:

$$
\begin{aligned}
{}^4\boldsymbol{f}_4 &= {}^4\boldsymbol{R}_5{}^5\boldsymbol{f}_5 + {}^4\boldsymbol{R}_8{}^8\boldsymbol{f}_8 + m_4{}^4\ddot{\boldsymbol{s}}_4, \qquad (11)\\
{}^4\boldsymbol{n}_4 &= {}^4\boldsymbol{R}_5{}^5\boldsymbol{n}_5 + {}^4\boldsymbol{R}_8{}^8\boldsymbol{n}_8 + {}^4\boldsymbol{I}_4{}^4\dot{\boldsymbol{\omega}}_4 + {}^4\boldsymbol{\omega}_4 \times ({}^4\boldsymbol{I}_4{}^4\boldsymbol{\omega}_4)\\
&\quad + {}^4\hat{\boldsymbol{s}}_4 \times (m_4{}^4\ddot{\boldsymbol{s}}_4) + {}^4\hat{\boldsymbol{p}}_5 \times ({}^4\boldsymbol{R}_5{}^5\boldsymbol{f}_5)\\
&\quad + {}^4\hat{\boldsymbol{p}}_8 \times ({}^4\boldsymbol{R}_8{}^8\boldsymbol{f}_8). \qquad (12)
\end{aligned}
$$

Similarly, force and torque of 11th, 14th and 17th links transmit to 10th link directly. Then, rotational motion equation of i-th link is obtained as Eq.(13) by making inner product of induced torque onto the i-th link's unit vector $\boldsymbol{e}_{z_i}$ around rotational axis:

$$
\tau_i = \boldsymbol{e}_{z_i}^T\ {}^i\boldsymbol{n}_i + d_i\dot{q}_i. \qquad (13)
$$

However, when the supporting-leg (1-st link) is slipping (prismatic joint), the torque onto the 1-st link can be calculated by following equation.

$$
f_1 = \boldsymbol{e}_{z_1}^T\ {}^1\boldsymbol{f}_1 + \mu_k\dot{y}_0. \qquad (14)
$$

Finally, we get motion equation with one leg standing as:

$$
\boldsymbol{M}(\boldsymbol{q})\ddot{\boldsymbol{q}} + \boldsymbol{h}(\boldsymbol{q}, \dot{\boldsymbol{q}}) + \boldsymbol{g}(\boldsymbol{q}) + \boldsymbol{D}\dot{\boldsymbol{q}} = \boldsymbol{\tau}, \qquad (15)
$$

Here, $\boldsymbol{\tau} = [f_1, \tau_1, \tau_2, \cdots, \tau_{17}]$ is input torque, $\boldsymbol{M}(\boldsymbol{q})$ is inertia matrix, both of $\boldsymbol{h}(\boldsymbol{q}, \dot{\boldsymbol{q}})$ and $\boldsymbol{g}(\boldsymbol{q})$ are vectors which indicate Coriolis force, centrifugal force and gravity. When the supporting-leg is slipping, the $\boldsymbol{D} = diag[\mu_k, d_1, d_2, \cdots, d_{17}]$ is a matrix which means coefficients of joint frictions including between foot and ground. And $\boldsymbol{q} = [y_0, q_1, q_2, \cdots, q_{17}]^T$ means the angle of joints and the relative position between foot and ground. When the supporting-leg is slipping, the variable vector $\boldsymbol{q}$ consists of $\boldsymbol{q} = [y_0, q_1, q_2, \cdots, q_{17}]^T$. The viscous friction of y-axis (slipping axis) can be described as $\mu_k\dot{y}_0$ that is included in left-side of Eq.(15), and the nonlinear force generated by reaction force to the supporting-leg f_{t0} is made by $f_{t0} = \mu_k f_{n0}$ where f_{n0} is normal force exerting to supporting-leg caused by dynamical coupling of the humanoid body given by Eqs.(9) and (10), and μ_k is dynamical friction coefficient.

This slipping motion state is depicted at right side of Fig.2. If $|\dot{y}_0| < \epsilon$ is satisfied, then the degree of motion, y_0, disappears, then the equation of motion transfers to the equation of motion that consists of $\boldsymbol{q} = [q_1, q_2, \cdots, q_{17}]^T$. On this state, static friction coefficient $\mu_s = 0.8$ is applied, and static friction force $f_{s0} = \mu_s f_{n0}$ exerts to the lateral direction of foot. When the exerting lateral force f_{y0} generated by dynamical coupling of humanoid body, that is ${}^i\boldsymbol{n}_i$ in Eq.(13) should satisfy $|f_{y0}| > |f_{s0}|$, then the slipping motion starts and the equation of motion, Eq.(15), is changed into the one with variables of $\boldsymbol{q} = [y_0, q_1, q_2, \cdots, q_{17}]^T$ again, which is depicted at the right state Fig.2.

The switching conditions were also described in previous studies about LCP (Linear Complementarity Problem) [26]. However, switching conditions in paper [26] is just for a model of ball, not for a robot which has a straight chain link structure. And the author's method is different with paper [26], when the humanoid's feet switch the slip or stick state, the equation of motion will also be switched as shown in Fig.2.

C. Constraint Conditions for Free-leg Model

Making Free-leg contact with ground, free-leg appears with the position z_h or angle q_e to the ground being constrained. Also, when free-leg's velocity in traveling direction $\dot{y}_h$ is less than 0.01[m/s], the free-leg will be constrained in acceleration by the static friction. The constraints of foot's z-axis position, heel's rotation and foot's y-axis position can be defined as C_1, C_2 and C_3 respectively, these constraints can be written as follow, where $\boldsymbol{r}(\boldsymbol{q})$ means the free-leg's heel or toe position in Σ_W.

$$
\boldsymbol{C}(\boldsymbol{r}(\boldsymbol{q})) = \begin{bmatrix} C_1(\boldsymbol{r}(\boldsymbol{q})) \\ C_2(\boldsymbol{r}(\boldsymbol{q})) \\ C_3(\boldsymbol{r}(\boldsymbol{q})) \end{bmatrix} = \boldsymbol{0} \qquad (16)
$$

Then, robot's equation of motion with external force f_{nz}, friction force f_t, external torque τ_n and external force f_{ny} corresponding to C_1, C_2 and C_3 can be derived as:

$$
\begin{aligned}
&\boldsymbol{M}(\boldsymbol{q})\ddot{\boldsymbol{q}} + \boldsymbol{h}(\boldsymbol{q}, \dot{\boldsymbol{q}}) + \boldsymbol{g}(\boldsymbol{q}) + \boldsymbol{D}\dot{\boldsymbol{q}}\\
&\qquad = \boldsymbol{\tau} + \boldsymbol{j}_{cz}^T f_{nz} - \boldsymbol{j}_t^T f_t + \boldsymbol{j}_r^T \tau_n + \boldsymbol{j}_{cy}^T f_{ny} \qquad (17)
\end{aligned}
$$

where $\boldsymbol{j}_{cz}$, $\boldsymbol{j}_t$, $\boldsymbol{j}_r$ and $\boldsymbol{j}_{cy}$ are defined as:

$$
\begin{aligned}
\boldsymbol{j}_{cz}^T &= \left(\frac{\partial C_1}{\partial \boldsymbol{q}^T}\right)^T \left(1/\left\|\frac{\partial C_1}{\partial \boldsymbol{r}^T}\right\|\right), \quad \boldsymbol{j}_t^T = \left(\frac{\partial \boldsymbol{r}}{\partial \boldsymbol{q}^T}\right)^T \frac{\dot{\boldsymbol{r}}}{\|\dot{\boldsymbol{r}}\|},\\
\boldsymbol{j}_r^T &= \left(\frac{\partial C_2}{\partial \boldsymbol{q}^T}\right)^T \left(1/\left\|\frac{\partial C_2}{\partial \boldsymbol{q}^T}\right\|\right), \quad \boldsymbol{j}_{cy}^T = \left(\frac{\partial C_3}{\partial \boldsymbol{q}^T}\right)^T \left(1/\left\|\frac{\partial C_3}{\partial \boldsymbol{q}^T}\right\|\right). \qquad (18)
\end{aligned}
$$

It is common sense that (i) f_{nz} and f_t are orthogonal, and (ii) value of f_t is decided by $f_t = K f_{nz}$ $(0 < K \leq 1)$. The differentiating Eq.(16) by time for two times, we can derive the constraint condition of $\ddot{\boldsymbol{q}}$.

$$
\left(\frac{\partial C_i}{\partial \boldsymbol{q}^T}\right)\ddot{\boldsymbol{q}} + \dot{\boldsymbol{q}}^T \left\{\frac{\partial}{\partial \boldsymbol{q}}\left(\frac{\partial C_i}{\partial \boldsymbol{q}^T}\right)\dot{\boldsymbol{q}}\right\} = 0 \quad (i = 1,\ 2) \qquad (19)
$$

Making the $\ddot{\boldsymbol{q}}$ in Eqs.(17) and (19) be identical, we can obtain the equation of contacting motion as follow.

$$\begin{bmatrix} \boldsymbol{M}(\boldsymbol{q}) & -(\boldsymbol{j}_{cz}^T - \boldsymbol{j}_t^T K) & -\boldsymbol{j}_r^T & -\boldsymbol{j}_{cy}^T \\ \partial C_1/\partial \boldsymbol{q}^T & 0 & 0 & 0 \\ \partial C_2/\partial \boldsymbol{q}^T & 0 & 0 & 0 \\ \partial C_3/\partial \boldsymbol{q}^T & 0 & 0 & 0 \end{bmatrix} \begin{bmatrix} \ddot{\boldsymbol{q}} \\ f_{nz} \\ \tau_n \\ f_{ny} \end{bmatrix}$$
$$= \begin{bmatrix} \boldsymbol{\tau} - \boldsymbol{h}(\boldsymbol{q}, \dot{\boldsymbol{q}}) - \boldsymbol{g}(\boldsymbol{q}) - \boldsymbol{D}\dot{\boldsymbol{q}} \\ -\dot{\boldsymbol{q}}^T \left\{ \dfrac{\partial}{\partial \boldsymbol{q}} \left(\dfrac{\partial C_1}{\partial \boldsymbol{q}^T} \right) \right\} \dot{\boldsymbol{q}} \\ -\dot{\boldsymbol{q}}^T \left\{ \dfrac{\partial}{\partial \boldsymbol{q}} \left(\dfrac{\partial C_2}{\partial \boldsymbol{q}^T} \right) \right\} \dot{\boldsymbol{q}} \\ -\dot{\boldsymbol{q}}^T \left\{ \dfrac{\partial}{\partial \boldsymbol{q}} \left(\dfrac{\partial C_3}{\partial \boldsymbol{q}^T} \right) \right\} \dot{\boldsymbol{q}} \end{bmatrix} \quad (20)$$

III. Validation of Model

A. Verification by Mechanical Energy

To verify this complex model, we use the mechanical energy conservation law. Because to verify the conservation of mechanical energy, the equation of motion must be correct. We make the model to do a free fall with the input torque $\boldsymbol{\tau}_i = 0$ and the viscous friction $\boldsymbol{D}_i = 0$. In this case, there is no friction. So, it will has no discharge of energy during free fall. During the motion the mechanical energy will be saved at the initial potential energy. To derive the mechanical energy, it is necessary to calculate all of the potential energy, rotational energy and translational energy.

B. Calculation of Mechanical Energy

It is necessary to calculate the height of the center of gravity of each link before the calculation of the potential energy. We use the homogeneous transformation matrix to calculate it as following equation.

$$^W z_{Gi} = {}^W z_i + \frac{^W z_{i+1} - {}^W z_i}{2} \quad (21)$$

Here, $^W z_{Gi}$ means the height of C.o.G of i-th link in world coordinate system $^W z_i$ is the height of the joint which seen from the world coordinate. So, we can calculate the potential energy as following equation.

$$E_p = \sum_{i=1}^{17} m_i {}^W z_i g \quad (22)$$

Here, E_p is the potential energy of the model. m_i is the mass of each link. g is the gravitational acceleration. Then, we can calculate the rotational energy as following equation.

$$E_k = \sum_{i=1}^{17} \frac{1}{2} {}^W \boldsymbol{\omega}_i^T {}^W \boldsymbol{I}_i {}^W \boldsymbol{\omega}_i \quad (23)$$

Here, E_k is the rotational energy of the model. $\boldsymbol{I}_i$ is the moment of inertia of each link. Then, we can also calculate the translational energy as following equation.

$$E_v = \sum_{i=1}^{17} \frac{1}{2} m_i {}^W \dot{\boldsymbol{r}}_{gi}^T {}^W \dot{\boldsymbol{r}}_{gi} \quad (24)$$

Here, E_v is the translational energy of the model, $\dot{\boldsymbol{r}}_{gi}$ is the translational velocity of C.o.G of i-th link. Finally, the mechanical energy can be derived as following equation.

$$E_Q = E_p + E_k + E_v \quad (25)$$

C. Simulation Including Stick-slip

A simulation with nonlinear friction between floor and foot has been prepared to examine a stick-slip motion that can verify the humanoid model. The experiment conditions are shown as follows. The state (stick or slip) of supporting-leg that is dominated by the stick-slip conditions are shown in Fig.2. When the driving force exerting to supporting-leg from dynamical coupling of humanoid nonlinear model f_{y0} is larger than the maximum static frictional force f_{s0}, the supporting-leg starts to slip. Here f_{n0} means the normal force exerting to the foot, and when the slip velocity of supporting-leg $|\dot{y}_0|$ is less than ϵ (a very small value $\epsilon = 0.001[m/s] = 1[mm/s]$ in this paper), the supporting-leg enters a stick state. During the supporting-leg in stick state, the coefficient of friction is set to $\mu_s = 0.8$, and when the supporting-leg is in slip state, the coefficient is set to $\mu_k = 0.4$. And the body of humanoid robot will fall freely without any viscous friction ($\boldsymbol{D} = \boldsymbol{0}$) and input torque ($\boldsymbol{\tau} = \boldsymbol{0}$).

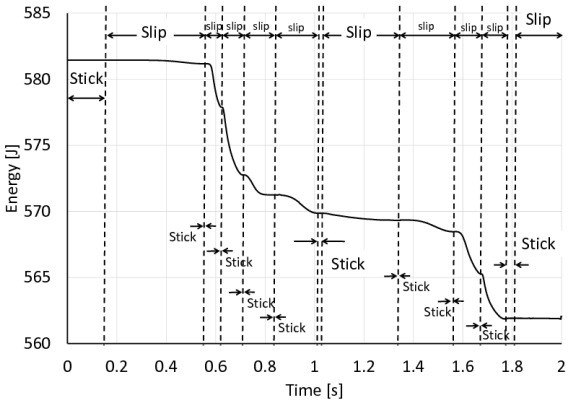

Fig. 3. Mechanical energy

$$E_{discharge} = \int_0^t \mu_k \dot{y}_0^2 dt \quad (26)$$

Fig.3 shows time profile of mechanical energy of humanoid's free-fall motion including the stick-slip motion, and Fig.4 shows the discharged energy caused by friction on floor, the calculation of discharged energy is shown in Eq.(26). Here, μ_k means the coefficient of friction when slipping, and when sticking the $E_{discharge}$ in Eq.(26) equal to zero since $\dot{y}_0$ is zero. In Figs.3 and 4, when the supporting-leg is in the state of stick, the total of mechanical energy is remained unchanged. And the mechanical energy discharges while the the supporting-leg is slipping, and the value of discharged energy in Fig.4 is consistent with the result in Fig.3.

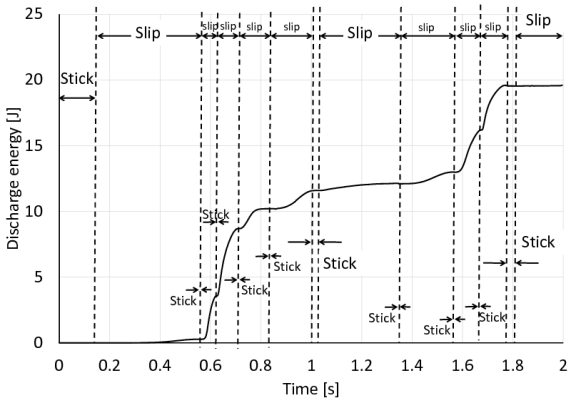

Fig. 4. Discharge of energy by friction

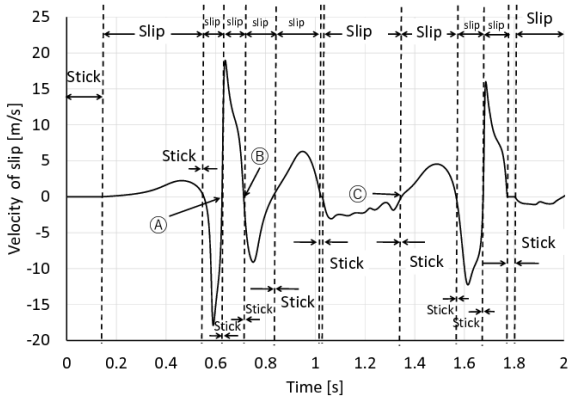

Fig. 5. Velocity of slip

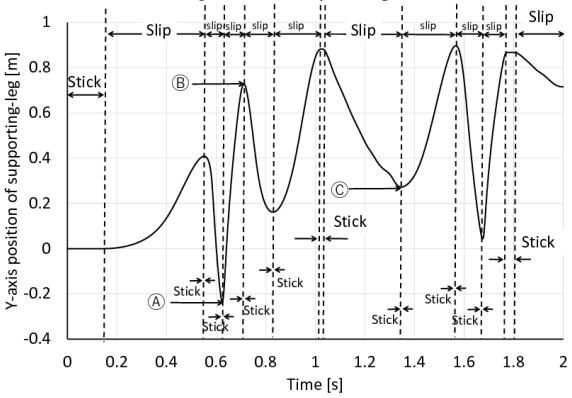

Fig. 6. y-position of supporting-leg

Furthermore the velocity and the y-axis position of supporting-leg are shown in Figs.5 and 6. Fig.5 shows that when the supporting-leg is in the state of stick, the velocity of slip equals to zero, and Fig.6 shows that the y-axis position is also not changed in time. And the discharge of energy depends on the velocity of slip. When the supporting-leg is slipping fast, the discharge of energy also gets a higher rate. Conversely, when supporting-leg is slipping very slow or stopping, the discharge of energy is also small or kept unchanged. So, from this simulation, it also can be seen that supporting-leg slip-stick model is feasible.

Fig.7 shows their shapes of the humanoid while the simulated motion proceeds as shown in Figs.3∼6. The configuration in Fig.7(a) was detected at the time designated by

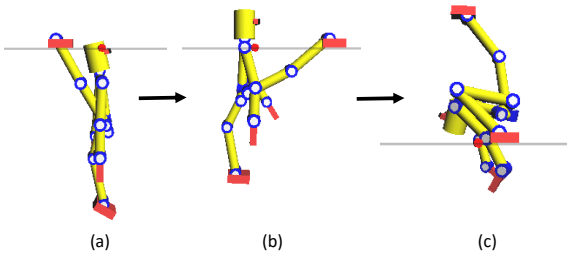

Fig. 7. Configurations during free-fall simulation shown in Fig.6, (a) the configuration at time Ⓐ designated in Fig.6, and (b) and (c) corresponds to time Ⓑ and Ⓒ

Ⓐ in Fig.5 and Fig.6, and also (b) and (c) are the shapes at Ⓑ and Ⓒ in the both figures.

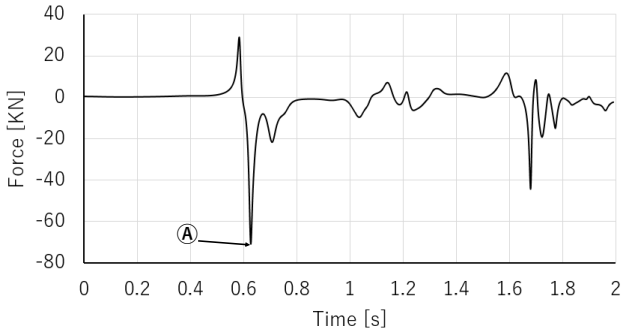

Fig. 8. Internal force f_{8z} of waist joint in z-axis (Σ_0).

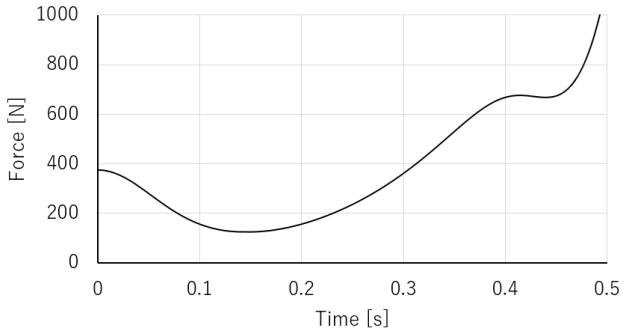

Fig. 9. Inter force f_{8z} of 0∼0.5[s] in Fig.8, Ⓐ shows the max value of f_{8z}.

Figs.8, 9 show the internal force f_{8z} of waist joint (8-th joint) in z-axis (Σ_0). Fig.9 is a part of Fig.8, it shows the internal force in the time of 0[s]∼0.5[s]. From Fig.9, when the robot is in initial state, the internal force of waist equals to 0.5G (half of weight of humanoid). When the robot starts to free-fall, the internal force becomes small and changing continually during free-fall motion. And at the time of Ⓐ in Fig.8, the internal force becomes maximum (100G). 100G is a very danger value for robot. This kind of internal force can broken the structure of waist joint even the linkage itself.

IV. CONCLUSIONS

In this paper, a dynamical model of humanoid robot including slipping of foot is proposed, that the equation of motion is derived by Newton-Euler method. And the model has been verified by using the mechanical energy conservation law. This model can be used to consider two different walking ways — using the slip positively like skating or controlling the slip to prevent falling. Furthermore the authors plan to extend the calculation method to the case of more than two constraint conditions, and evaluate it by simulations, which may be useful for the analyses for dynamical sequences of humanoid robot when it is falling down to the ground.

REFERENCES

[1] S. Kajita, M. Morisawa, K, Miura, S. Nakaoka, K. Harada, K. Kaneko, F. Kanehiro and K. Yokoi, "Biped Walking Stabilization Based on Linear Inverted Pendulum Tracking," *Proceedings of IEEE/RSJ International Conference on Intelligent Robots and Systems*, pp.4489–4496, 2010.

[2] H. Dau, C. Chew and A. Poo, "Proposal of Augmented Linear Inverted Pendulum Model for Bipedal Gait Planning," *Proceedings of IEEE/RSJ International Conference on Intelligent Robots and Systems*, pp.172–177, 2010.

[3] J.H. Park and K.D. Kim, "Biped walking robot using gravity-compensated inverted pendulum mode and computed torque control," *Proceedings of IEEE International Conference on Robotics and Automation*, Vol.4, pp.3528–3593, 1998.

[4] P.B. Wieber, "Trajectory free linear model predictive control for stable walking in the presence of strong perturbations," *Proceedings of International Conference on Humanoid Robotics*, 2006.

[5] P.B. Wieber, "Viability and predictive control for safe locomotion," *Proceedings of IEEE/RSJ International Conference on Intelligent Robots and Systems*, 2008.

[6] A. Herdt, N. Perrin and P.B. Wieber, "Walking without thinking about it," *Proceedings of IEEE/RSJ International Conference on Intelligent Robots and Systems*, pp.190–195, 2010.

[7] Y. Huang, B. Chen, Q. Wang, K. Wei and L. Wang, "Energetic efficiency and stability of dynamic bipedal walking gaits with different step lengths," *Proceedings of IEEE/RSJ International Conference on Intelligent Robots and Systems*, pp.4077–4082, 2010.

[8] M. Sobotka and M. Buss, "A Hybrid Mechatronic Tiliting Robot: Modeling, Trajectories, and Control," *Proceedings of the 16th IFAC World Congress*, 2005.

[9] T. Wu, T. Yeh and B. Hsu, "Trajectory Planning of a One-Legged Robot Performing Stable Hop," *Proceedings of IEEE/RSJ International Conference on Intelligent Robots and Systems*, pp.4922–4927, 2010.

[10] Y. Nakamura and K. Yamane, "Dynamics of Kinematic Chains with Discontinuous Changes of Constraints—Application to Human Figures that Move in Contact with the Environments—," *Journal of RSJ*, Vol.18, No.3, pp.435–443, 2000 (in Japanese).

[11] J.Nishiguchi, M.Minami, A.Yanou, "Iterative calculation method for constraint motion by extended Newton-Euler method and application for forward dynamics," *Transactions of the JSME*, Vol.80, No.815, 2014.

[12] H. Hemami and B.F. Wyman, "Modeling and Control of Constrained Dynamic Systems with Application to Biped Locomotion in the Frontal Plane," *IEEE Transactions on Automatic Control*, AC-24-4, pp.526–535, 1979.

[13] B. Siciliano, O. Khatib (Eds.), "Handbook of Robotics," Section Kinematic Loops, *Springer*, 2008.

[14] T. Feng, J. Nishiguchi, X. Li, M. Minami, A. Yanou and T. Matsuno, "Dynamical Analyses of Humanoid's Walking by using Extended Newton-Euler Method," *20st International Symposium on Artificial Life and Robotics(AROB 20st)*, 2015.

[15] Yosuke Kobayashi, Mamoru Minami, Akira Yanou, Tomohide Maeba, "Dynamic Reconfiguration Manipulability Analyses of Humanoid Bipedal Walking" *IEEE International Conference on Robotics and Automation (ICRA)*, p4764-4769, 2013.

[16] T.Aoyama, Y.Hasegawa, K. Sekiyama and T.Fukuda, "tabilizing and Direction Control of Efficient 3-D Biped Walking Based on PDAC," *2009 IEEE/ASME transactions on mechatronics*, pp.712-718, 2009.

[17] T. Sugihara and Y. Nakamura, "Whole-body Cooperative COG Control through ZMP Manipulation for Humanoid Robots," *Proceedings of the 2nd International Symposium on Adaptive Motion of Animals and Machines*, SaP-III-4, 2003.

[18] Christine Chevallereau, J. W. Grizzle, Ching-Long Shih, "Asymptotically Stable Walking of a Five-Link Underactuated 3-D Bipedal Robot," *IEEE transactions on robotics*, VOL. 25, NO. 1, FEBRUARY 2009.

[19] S. Kajita, K. Kaneko, K. Harada, F. Kanehiro, K. Fujiwara, and H. Hirukawa, "Biped Walking on a Low Friction Floor," *Proc. of the IEEE/RSJ International Conference on Intelligent Robots and Systems*, pp. 3546-3552, 2004.

[20] K. Kaneko, F. Kanehiro, S. Kajita, M. Morisawa, K. Fujiwara, K. Harada, and H. Hirukawa, "Slip Observer for Walking on a Low Friction Floor", *Proc. of the IEEE/RSJ International Conference on Intelligent Robots and Systems*, pp. 634-640, 2005.

[21] G. N. Boone and J. K. Hodgins, "Slipping and Tripping Reflexes for Bipedal Robots," *Autonomous Robots*, Vol. 4, pp. 259-271, 1997.

[22] J. H. Park and O. Kwon, "Reflex Control of Biped Robot Locomotion on a Slippery Surface," *Proc. of the IEEE International Conference on Robotics and Automation*, pp. 4134-4139, 2001.

[23] Ueda Yoshisuke, Henmi Masanori, "An experimental and analytical study on Stick-Slip motions," *Technical Report of lEICE*, CAS Vol.96, 41-48, 1996.

[24] Luis R. Tokashiki, Toshinori Fujita, Toshiharu Kagawa, "Stick-Slip Motion in Pneumatic Cylinders Driven by Meter-out Circuit 1st Report, Friction Characteristics and Stick-Slip Motion ," *Transactions of The Japan Hydraulics & Pneumatics Society*, Vol. 30, No. 4, p110-117, 1999.

[25] Ken Nakano, "A Guideline of Machinary Design for Preventing Stick-Slip" *Nippon Gomu Kyokaishi*, Vol. 80, No. 4, p134-139, 2007.

[26] D. Stewart and J. Trinkle, " An implicit time-stepping scheme for rigidbody dynamics with inelastic collisions and Coulomb friction, " Int. J. of Numerical Methods Engineering, vol. 39, pp. 2673-2691, 1996.

[27] M. Kouchi, M. Mochimaru, H. Iwasawa and S. Mitani, "Anthropometric database for Japanese Population 1997-98," *Japanese Industrial Standards Center (AIST, MITI)*, 2000.